Electrospun Nanofibrous Membranes with Essential Oils for Wound Dressing Applications

Kyung Lee and Seungsin Lee*

Department of Clothing and Textiles, Yonsei University, Seoul 03722, Korea
(Received March 23, 2019; Revised October 5, 2019; Accepted October 12, 2019)

Abstract: To develop bioactive and interactive wound-dressing materials based on natural products, poly(vinyl alcohol) (PVA) nanofibrous membranes containing plant-derived essential oils were fabricated and their potential applications for wound dressing were examined. Since essential oils, particularly palmarosa oil and phytoncide oil, possess natural antimicrobial and anti-inflammatory properties and are ecofriendly, they were chosen as bioactive agents to be incorporated into the nanofiber matrix. Antimicrobial efficacy, air/moisture vapor transport, and water uptake properties of the composite membranes were assessed to find suitable processing conditions for effective wound care. Palmarosa oil or phytoncide oil was incorporated into the core of PVA nanofibers via emulsion electrospinning. The PVA-based composite nanofibrous membranes were heat-treated to increase their stability in aqueous environments. Qualitative and quantitative antimicrobial assessments showed that the membranes containing palmarosa oil possessed superior antimicrobial effects against *Staphylococcus aureus* and *Candida albicans* over the membranes containing phytoncide oil. Air/moisture vapor transport and water uptake properties were assessed for the PVA-based composite membranes having two levels of web area density to find suitable conditions for creating an optimal wound-healing environment. The composite nanofibrous membranes, which had a web area density of 3 g/m^2, provided reasonable levels of gas and moisture vapor permeability for effective wound care and possessed water uptake ability to allow exudate absorption. These results demonstrate that the electrospun core/sheath structured PVA nanofibrous membranes containing palmarosa oil have high potential as bioactive wound-dressing materials.

Keywords: Nanofibrous membrane, Palmarosa oil, Phytoncide oil, Emulsion electrospinning, Wound dressing

Introduction

The need for innovative medical products that are beneficial to patient needs is constantly rising with the growing expectations in the medical and health care sector. A wound dressing provides a protective barrier to the wound to assist in wound healing and prevent bacterial infections [1]. To provide an optimal environment for wound healing, an ideal dressing is expected to protect the wound from bacterial invasion, maintain a moist environment by minimizing evaporative water loss from the wound, absorb and control exudates, reduce infection risk, and accelerate wound healing [2]. Nontoxicity to mammalian cells and flexibility to adhere well to the underlying topography are also essential requirements [1]. To meet these requirements, a desirable wound-dressing material should have antimicrobial efficacy, moderate air and vapor permeability, high absorbency, high flexibility, and nontoxicity [3].

Electrospun polymeric nanofibrous membranes have attracted great interest in biomedical applications including wound dressing, drug delivery, and medical implants because of their unique properties of exceptionally small pore size, high specific surface area, and high porosity. The innate structural advantages of electrospun nanofibrous membranes allow them to act as effective and breathable barriers against penetration from external bacteria, fungi, and other contaminants. Furthermore, membranes comprising numerous nanofibers possess flexibility with negligible

roughness [4], which is important for dressing comfort and fit. These unique features of nanofibrous membranes make them excellent candidates for use in medical textiles such as wound dressings.

In recent years, bioactive and interactive wound dressings, which contain therapeutic or antimicrobial agents to further promote wound healing, have attracted considerable interest [1,2]. In addition to maintaining a moist wound environment, bioactive wound dressings create an optimum micro-environment for wound healing via a sustained release of bioactive agents. The incorporation of various natural functional materials into the matrix of nanofibers for biomedical applications has been previously studied owing to their nontoxicity and ecofriendliness [5-9]. Sarkar *et al.* [5] investigated the antioxidant, antibacterial, and anti-inflammatory performance of honey-incorporated electrospun nanofibers for wound regeneration. Rieger and Schiffman [6] demonstrated the electrospinning of cinnamon essential oil in a chitosan/poly(ethylene oxide) maxtrix and obtained nanofibers with high antimicrobial efficiency against *Escherichia coli* and *Pseudomonas aeruginosa*. In a study by Wang and Mele [7], essential oils of clary sage and black pepper were incorporated in poly(lactic acid) nanofibers, and the effects of essential oils on the morphology of electrospun fibers were investigated. The addition of essential oils generated fibers with either wrinkled (for clary sage oil) or nano-textured surfaces (for black pepper oil), exhibiting antibacterial activity against *Escherichia coli* and *Staphylococcus epidermidis*. Rafiq *et al.* [8] investigated the incorporation of three different essential oils such as

cinnamon, clove, and lavender in sodium alginate/poly(vinyl alcohol) nanofibers and examined their antibacterial properties against *Staphylococcus aureus*. The authors reported that cinnamon oil-loaded nanofibers showed the best antibacterial effects among the three oils that were analyzed.

Although previous studies suggest that natural functional materials including essential oils impart bioactivities to electrospun fibers, which makes them excellent candidates for advanced wound dressings, they mainly focused on the fabrication of composite nanofibers containing natural substances and demonstration of their antibacterial effects. A more comprehensive study is needed to explore the potential of composite nanofibrous membranes loaded with natural substances as bioactive and interactive wound dressings, considering not only the antimicrobial efficiency but also their air/moisture vapor transport, water uptake properties and so on.

Essential oils, which are volatile organic compounds obtained from plants, possess various bioactivities such as antimicrobial, antifungal, antioxidant, and anti-inflammatory properties [10,11]. Therefore, they are extensively used in various applications in the pharmaceutical, cosmetic, skin care, and food industries. The essential oil derived from Palmarosa grass (*Cymbopogon martinii*) shows antimicrobial activity against a wide range of bacteria, including antibiotic-resistant species and fungal species, mainly because it is rich in geraniol and geranyl acetate [12]. The phytochemical analysis of palmarosa oil indicated the presence of geraniol (68-84 %) and geranyl acetate (2-16 %) as the major components [13]. Geraniol is known for its biochemical and pharmacological properties, such as antifungal, antiseptic, and repellent properties in addition to its rose-like aroma and taste [14]. Therefore, palmarosa oil is used for gargles as a treatment for throat infections, for manufacture of soaps and perfumes, and in skin care [15]. Phytoncides, which are terpene-based complex compounds produced by various trees and plants, are known for their natural antimicrobial properties and protect trees and plants against harmful microorganisms and insects [16]. Among the phytoncide oils extracted from various plants, the phytoncide oil from hinoki cypress (*Chamaecyparis obtusa*) exhibits strong physiological effects such as antimicrobial, anti-inflammatory, and stress-relieving effects [17,18]. The major components of phytoncide oil are monoterpenes and oxygenated monoterpenes including limonene, sabinene, α-terpinyl acetate, pinene, and bornyl acetate [19-21]. Individual oil components, such as limonene, sabinene, pinene, and bornyl acetate were found to exhibit antibacterial activities against a range of strains [22]. Therefore, it is worth incorporating palmarosa and phytoncide oils into the nanofiber matrix to develop bioactive wound-dressing materials for controlling secondary infection or skin disorders such as irritation, allergic responses, and dermatitis.

Emulsion electrospinning is a simple method to create core/sheath structured nanofibers from a single-nozzle electrospinning setup using emulsion as the working liquid [23]. In this method, an emulsion containing two immiscible liquid phases is electrospun using a single-nozzle electrospinning setup. Core/sheath structures are generated because of the stretching and coalescence of the emulsion during the electrospinning process. This is associated with the differences in volatility between the two liquid phases. When sufficiently high voltage is applied to the needle, a spinning solution suspended at the needle tip is stretched in a jet form. Because the solvent of the polymer solution forming the continuous phase evaporates more rapidly, the viscosity of the continuous phase becomes higher than that of the dispersed phase. This makes the emulsion droplets move inward during electrospinning and merge in the core of fiber, which is called "evaporation and stretching induced de-emulsification" [24]. The core/sheath configuration enables the embedding of drugs or functional materials in the fiber core for a sustained release of the embedded components.

Owing to its nontoxicity, biocompatibility, biodegradability, and chemical resistance, poly(vinyl alcohol) (PVA) is widely used in biomedical applications, including wound dressings, drug delivery systems, and dialysis membranes [25,26]. PVA is water soluble, and it enables "green electrospinning" using water as the electrospinning medium. However, post-treatment is necessary to stabilize the fibers in a moist environment such as a wounded area. Although PVA can be chemically crosslinked using organic solvents such as formaldehyde or glutaraldehyde, this method may limit the use in biomedical applications where the toxicity of organic solvents could be highly critical. Alternatively, a few studies [27,28] have discussed the crosslinking of PVA fibers physically through heat treatment, which is an environmentally friendly method that does not require the use of toxic chemicals. Therefore, in this study the heat-treatment method was used without any chemical treatment to increase the aqueous stability of PVA-based membranes for wound-dressing applications.

Although a number of studies have focused on fabricating functional composite nanofibers having various active components for biomedical applications, few studies have investigated the various aspects required for wound-dressing applications, including air/moisture vapor permeability, fluid absorbency, pore size distribution, and antimicrobial efficacy, which are critical factors in creating an optimal environment for wound healing. In this study, we focused on the manufacture of bioactive wound-dressing materials that meet the requirements for effective wound care in various aspects. Core/sheath structured PVA nanofibrous membranes containing palmarosa and phytoncide oils were fabricated, respectively. Their antimicrobial properties were evaluated *in vitro* both qualitatively and quantitatively. The composite nanofibrous membranes having different levels of web area density were evaluated for water vapor transmission rate, air

permeability, water uptake properties, and pore size distribution to examine the feasibility of the membranes for use in wound dressing and to find suitable processing conditions for such applications.

Experimental

Materials

PVA (>99 % hydrolyzed, Mw=89,000-98,000) was supplied by Sigma Aldrich Co. (USA). Pure *Chamaecyparis obtusa* phytoncide oil was purchased from Ecomist Co. (Korea), and palmarosa oil was purchased from Neumond Co. (Germany). Nonionic surfactant, Tween 80, was supplied by Kao Co. (Japan). Tween 80 was chosen as a surfactant based on its hydrophilic-lipophilic balance values [29] to stabilize oil-in-water (O/W) emulsions. Nile red, a lipophilic and fluorescent dye, was obtained from Sigma Aldrich Co. (USA) and used for confocal laser scanning microscopy (CLSM) analysis.

Electrospinning Process

An O/W-type emulsion comprising PVA solution as the water phase and essential oils as the oil phase was prepared before electrospinning. PVA powders were dissolved in distilled water at 80 °C for 6 h, followed by addition of essential oils and Tween 80 to the PVA solutions. Emulsions were then stirred using a vortex mixer for over 2 h. The PVA concentrations were set within the range of 11-13 wt%. The concentrations of essential oils and Tween 80 were set within the range of 3-5 wt% and 0.71-0.93 wt%, respectively.

Electrospinning was performed in a single-nozzle electrospinning setup (NNC-ESP200R2, NanoNC Co., Korea) under various spinning conditions to optimize the conditions for fabricating core/sheath structured nanofibers. The system comprised a syringe, a syringe pump, a high-voltage power supply, and a grounded collector. A computer-aided system was used to control the nozzle system and the collector, which run lengthwise and crosswise, respectively, facilitating the fabrication of uniform nanofibrous membranes. Emulsions were put into a plastic syringe, and an electrode was clipped to the needle. The syringe pump delivered the emulsions at a constant volumetric feed rate ranging from 0.2 to 1.8 m*l*/h. A high voltage of 21-25 kV was applied to the needle. The needle gauges used were 23 (0.33 mm *i.d.*) and 27 (0.20 mm *i.d.*). The tip-to-collector distance was maintained at 18 cm. As the high voltage was applied to the needle, nanocomposite fibers were electrospun and deposited directly onto a substrate mounted on the grounded collector. The substrate fabric was 100 % cotton gauze; it weighed 30.4 g/m^2 with a fabric count of 54×40 (W×F)/5 cm.

Colloidal Properties

The emulsion viscosity was measured using a rheometer (ARES, Rheometric Scientific Co., USA) under shear rates of 100 s^{-1} at a controlled temperature of 25 °C. A multi-range conductivity meter (HI 8633, Hanna Instruments, Romania) was used to measure the conductivity of emulsions. A tensiometer (KSV Sigma 702, Biolin Scientific Co., Finland) was used for the measurement of surface tension.

Fiber Morphology

The morphology of the electrospun nanocomposite fibers was examined using a field emission scanning electron microscope (FE-SEM; Hitachi Model S-4200, Nissei Sangyo, Japan) after sputter-coating with Pt/Pd. Fiber diameters were measured from the SEM micrographs using image analysis software (ImageJ, National Institutes of Health, USA). The average fiber diameter was obtained on a minimum of 45 measurements from different parts of each sample.

A transmission electron microscope (TEM; JEM 1010, JEOL, Japan) and a confocal laser scanning microscope (CLSM; CLSM 700, Carl Zeiss, USA) were used to further characterize the morphology of the bicomponent fibers. For CLSM analysis, a lipophilic dye, Nile red, was used as a fluorescent marker to track the oil within the fibers. Essential oils were labeled by dissolving 0.01 g/m*l* Nile red in the oils before electrospinning. Emulsions containing Nile red-labeled oils were electrospun, and the nanocomposite fibers were examined under a CLSM to visualize the distribution of Nile red-labeled oils within the fibers. An excitation wavelength of 488 nm was used for the analysis.

Heat Treatment

PVA nanofibrous membranes containing essential oils were heat-treated at 170 °C for 5 min to increase the aqueous stability of the membranes. The heat-treatment conditions were chosen based on preliminary experimental trials. To confirm whether the heat treatment stabilized the PVA-based membranes against dissolution in water, both heat-treated and untreated nanofibrous membranes were immersed in water at 37 °C for 1 h, considering the environment of application under the skin contact temperature. Then, the morphology of the membranes was examined using an FE-SEM to examine the effect of heat treatment.

Fourier Transform Infrared Spectroscopy (FT-IR) Measurements

To verify the presence of essential oils within the composite fibers and whether the chemical structure was preserved after electrospinning and heat-treatment processes, infrared spectra of the composite fibers before and after heat treatment were collected using an FT-IR spectrometer (Vertex 70, Bruker Co., Germany). The samples were analyzed using the attenuated total reflectance (ATR) mode in the range of 400-4000 cm^{-1}.

Assessment of Antimicrobial Efficacy

The antimicrobial activities of PVA nanofibrous membranes loaded with essential oils were evaluated both qualitatively and quantitatively. The qualitative assessment was performed in accordance with ISO 20645:2010 (Textile fabrics—Determination of antibacterial activity—Agar diffusion plate test). In this method, the antimicrobial activity of a textile sample was determined by observing the hindrance of bacterial growth underneath the sample and around its edges. Inhibition zones were determined using the following formula:

$$H = \frac{D - d}{2} \tag{1}$$

where H is the inhibition zone, D is the total diameter of the specimen and the inhibition zone, and d is the diameter of the specimen.

The quantitative assessment was performed according to the American Association of Textile Chemists and Colorists (AATCC) Test Method 100-2012 (Assessment of antibacterial finishes on textile materials). The reduction percentage of test organisms after contacting the sample for 24 h was determined using the following formula:

$$R \ (\%) = \frac{B - A}{B} \times 100 \tag{2}$$

where R is the reduction rate of the number of colonies, A is the number of bacterial colonies in the flask containing treated samples after a specified contact time, and B is the number of bacterial colonies in the flask before the addition of the treated samples.

For the qualitative and quantitative antimicrobial assessments, specimens having a web area density of 3 g/m^2 were prepared, and heat treatment was applied before the antimicrobial assessment. Two kinds of strains, *Staphylococcus aureus* (ATCC 6538, Gram-positive bacterium) and *Candida albicans* (ATCC 10231, Eumycetes), were used as the representative microorganisms to challenge the antimicrobial functions of the PVA nanofibrous membranes containing essential oils.

Air and Moisture Vapor Transport Properties

Air permeability and water vapor transmission rate were evaluated for the composite membranes having two levels of web area density (3 and 6 g/m^2) before and after heat treatment to examine the effect of web area density and heat treatment on air/moisture vapor transport properties of the material. The level of web area density was controlled by the electrospinning duration. Air permeability was measured in accordance with ASTM D737-04 (Standard test method for air permeability of textile fabrics) using a Frazier Air Permeability Tester. The testing area was 38 cm^2, and the pressure drop used was 125 Pa.

Water vapor transmission rate was measured according to

ASTM E96/E96M-16 (Standard test methods for water vapor transmission of materials). The test specimen was sealed to the open mouth of a test dish containing distilled water. The weighing determined the rate of vapor movement through the specimen from the water to a controlled atmosphere, in which the air temperature was 32±1 °C and the relative humidity was 50±2 %.

Pore Size Distribution

Specimens having two levels of web area density (3 and 6 g/m^2) were prepared, and pore size distributions of the as-spun and heat-treated composite nanofibrous membranes were measured to examine the effects of heat treatment and web area density on the pore size. Pore size distribution was measured using a capillary flow porometer (Model CFP-1500-AE, Porous Materials, Inc., USA). Gas flow rates through wet and dry samples versus differential pressure were measured, and pore diameters of through-pores at the most constricted part of the pore were determined.

Water Uptake Ability

For evaluating water uptake ability, specimens having two levels of web area density (3 and 6 g/m^2) were prepared. As PVA is water soluble, all samples were thermally treated before the water uptake assessment. Dry samples were cut into square shapes of 1 cm×1 cm and weighed. Samples were then immersed in distilled water for 2 h and weighed after surplus water on the membrane surface was removed using filter paper. The water uptake ability was calculated using the following formula:

$$\text{Water uptake ability } (\%) = \frac{W_{wet} - W_{dry}}{W_{dry}} \times 100 \tag{3}$$

where W_{dry} and W_{wet} are the masses of membranes before and after immersion in water, respectively.
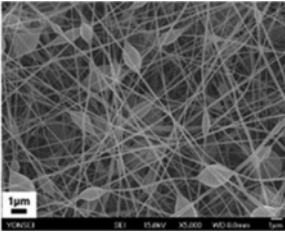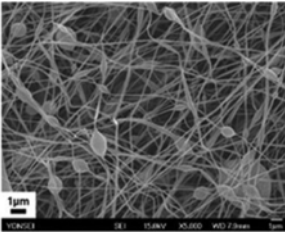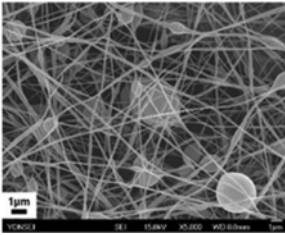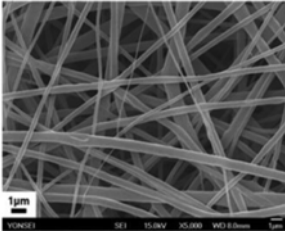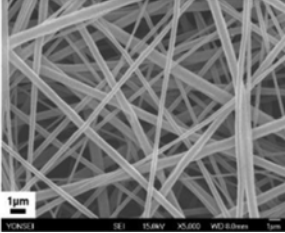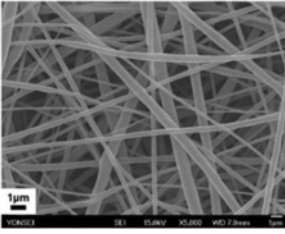
Statistical Analysis

Statistical analysis was performed to determine the differences in air/moisture vapor transport properties between the as-spun and heat-treated specimens and between the two levels of web area density using the SPSS 18.0 package program. We performed t-tests at a 95 % confidence level (p=0.05) to examine the significant difference in the means of the variables.
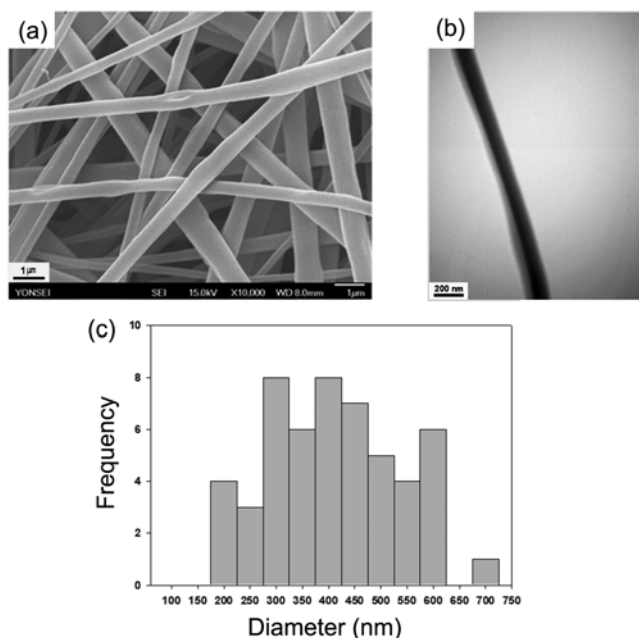
Results and Discussion

Morphology of PVA Nanofibers Containing Essential Oil

To produce core/sheath structured nanocomposite fibers by emulsion electrospinning, an appropriate set of parameters for the emulsion and processing should be selected. On the basis of a previous study [30], the PVA concentrations were set within the range of 11-13 wt%. The concentrations of essential oils and Tween 80 were set within the range of

Table 1. SEM images of phytoncide oil/PVA nanofibers produced using different emulsion formulations and processing conditions

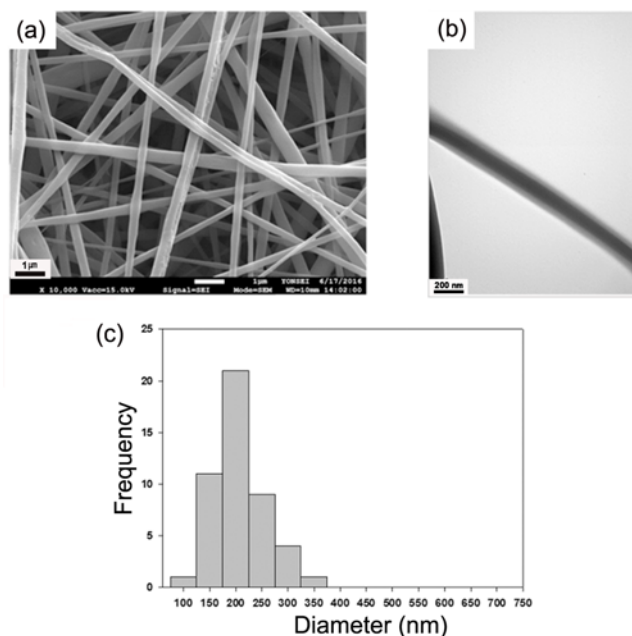| PVA concentration (wt%)	Phytoncide oil concentration (wt%)	Tween 80 concentration (wt%)	Feed rate (m*l*/h)	Needle gauge	Fiber morphology
11	3	0.79	0.2	23	
			0.8	23	
			1.8	27	
13	5	0.93	0.2	23	
			0.8	23	
			1.8	23	

Figure 1. (a) SEM image, (b) TEM image, and (c) fiber size distribution of the phytoncide oil/poly(vinyl alcohol) (PVA) nanocomposite fibers.

Figure 2. (a) SEM image, (b) TEM image, and (c) fiber size distribution of the palmarosa oil/PVA nanocomposite fibers.

3-5 wt% and 0.71-0.93 wt%, respectively. Emulsions having different emulsion formulations were electrospun under various spinning conditions to find suitable conditions for fabricating core/sheath structured nanofibers. Table 1 presents the selected SEM images of PVA nanofibers containing phytoncide oil produced from different emulsion formulations and spinning conditions. Based on the preliminary experiments, the suitable emulsion formulations and processing conditions for fabricating uniform composite nanofibers were determined considering the fiber morphology and ease of spinnability.

Figure 1(a) shows an SEM image of PVA nanocomposite fibers loaded with phytoncide oil obtained from the emulsion containing 13 wt% PVA, 5 wt% phytoncide oil, and 0.93 wt% surfactant (*i.e.*, the oil accounted for 26 wt% of the fiber mass). The emulsion yielded relatively straight nanocomposite fibers having an average diameter of 429± 63 nm. Suitable spinning conditions for fabricating bead-free composite fibers were a feed rate of 0.2 m*l*/h, a voltage of 25 kV, and a collecting distance of 18 cm through a 23-gauge needle. The morphology of the fibers was further examined using a TEM to verify the core/sheath structure of the emulsion electrospun nanofibers. A TEM image of the composite fiber loaded with phytoncide oil (Figure 1(b)) shows a uniform core and sheath structure as indicated by the dark and bright regions along the fiber length.

The SEM image of PVA nanocomposite fibers loaded with palmarosa oil is shown in Figure 2(a). The fibers were electrospun under the same processing conditions from the
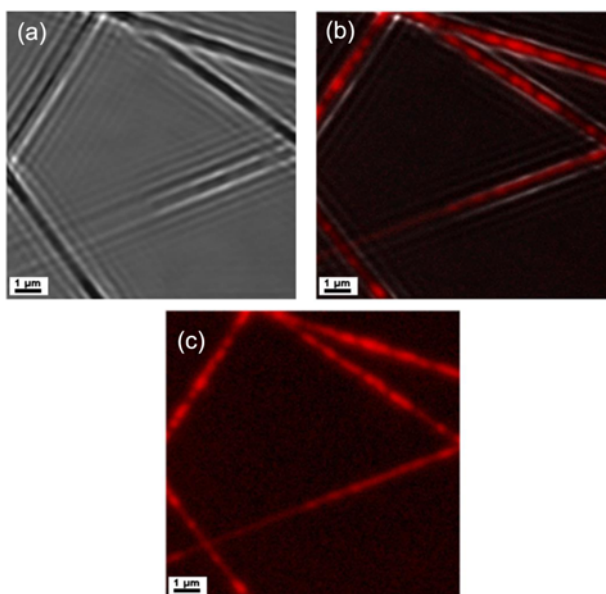
same ratios of emulsion formulations as those of the fibers containing phytoncide oil. Bead-free composite fibers were obtained, which had relatively smooth surfaces and an average diameter of 231±26 nm. A TEM image of the composite fiber loaded with palmarosa oil (Figure 2(b)) illustrates a well-aligned core/sheath structure in which palmarosa oil was efficiently incorporated into the fiber core. Overall, composite fibers loaded with palmarosa oil showed smaller fiber sizes and a narrower fiber size distribution than those loaded with phytoncide oil, as depicted in Figures 1(c) and 2(c).

The differences in fiber dimensions between phytoncide oil/PVA nanofibers and palmarosa oil/PVA nanofibers may be attributed to the colloidal properties. Table 2 summarizes the emulsion composition and properties such as viscosity, electrical conductivity, and surface tension. The phytoncide oil/PVA emulsion showed higher viscosity and lower conductivity than that of the palmarosa oil/PVA emulsion. Generally, higher viscosity and lower electrical conductivity of electrospinning solutions result in the insufficient stretching of the electrified jet; therefore, thicker fibers are produced during electrospinning [31]. Thus, the larger fiber diameter of phytoncide oil/PVA nanofibers may be attributed to the influence of higher viscosity and lower electrical conductivity of the precursor emulsion. These findings are in agreement with previous studies that reported similar observations [32,33].

A confocal laser scanning microscope was used to confirm the core/sheath structure and to visualize the distribution of essential oils within the fibers. A lipophilic dye, Nile red,

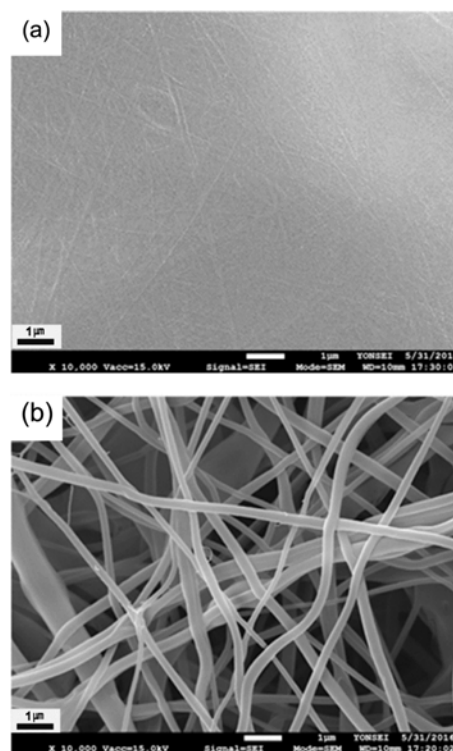**Table 2.** Emulsion compositions and their viscosity, electrical conductivity, and surface tension

Emulsion or solution	PVA concentration (wt%)	Oil concentration (wt%)	Viscosity (Pa·s)	Electrical conductivity (μS/cm)	Surface tension (mN/m)
PVA	13	-	0.82	503	66.1
Palmarosa oil/PVA	13	5	0.92	493	30.5
Phytoncide oil/PVA	13	5	1.23	476	33.0

Figure 3. Confocal laser scanning microscope (CLSM) images of core/sheath structured PVA nanofibers containing palmarosa oil (images of the same fibers); (a) without excitation, (b) with excitation, and (c) with superimposed excitation light.

Figure 4. SEM images of electrospun PVA nanofibrous membranes containing palmarosa oil after immersion in water; (a) as-spun and (b) heat-treated.

was used to label the non-fluorescent essential oils. As presented in Figure 3, the Nile red-labeled essential oils emitted strong fluorescence at an excitation wavelength of 488 nm, shown in red color. The CLSM images clearly show that the core/sheath structure was formed and palmarosa oil was successfully incorporated into the core of fibers, being distributed continuously throughout the core.

Effect of Heat Treatment

We thermally treated PVA nanofibrous membranes containing essential oils at 170 °C for 5 min and then immersed them in water at 37 °C for 1 h to examine the changes in their morphologies. As shown in Figure 4(a), the as-spun PVA nanofibers containing palmarosa oil completely lost their fibrous structure after immersion in water. In contrast, the heat-treated nanocomposite fibers preserved their fibrous structure after exposure to an aqueous environment (Figure 4(b)). The average diameters of the heat-treated nanocomposite fibers before and after immersion in water were 233±27 nm and 236±28 nm,

respectively. Although there was a slight increase in the fiber diameter after exposure to water, no considerable changes were observed in the fiber diameter.

Similar results were exhibited for the PVA nanofibrous membranes containing phytoncide oil, *i.e.*, the heat treatment stabilized the PVA composite fibers containing phytoncide oil against dissolution in water (results not shown). The thermal treatment of PVA above its glass transition temperature was reported to stabilize the structure by increasing the polymer crystallinity [28]. Heat treatment induces hydrogen bonds and hence facilitates the formation of crystallites; the water resistance of PVA can be achieved by a physical crosslinking network among the crystallites formed by heat treatment [34]. The heat-treatment conditions used herein were shown to be effective in stabilizing the PVA-based composite nanofibers against disintegration in water.

Chemical Component Analysis

The chemical structures of the PVA nanofibrous membranes containing essential oils were further characterized by FT-IR before and after heat treatment. Figure 5 presents FT-IR spectra for heat-treated pristine PVA nanofibers, palmarosa oil, and PVA nanofibers containing palmarosa oil before and after heat treatment. For pure palmarosa oil, characteristic bands were observed at 3367 cm^{-1} (OH group), 2967 and 2919 cm^{-1} (C-H aliphatic stretch), 1722 cm^{-1} (C=O stretch for the acid group), and 1669 cm^{-1} (C=C conjugated diene), as shown in Figure 5(c). Among these peaks, the peaks attributed to the C=O stretch for the acid group and C=C conjugated diene did not exist in the pristine PVA nanofibers (Figure 5(d)), but they were observed in the spectra of PVA nanofibers containing palmarosa oil before and after heat treatment (Figure 5(b) and (a)). This result further confirms that palmarosa oil was incorporated into the PVA nanofibrous matrix and maintained the molecular structure after the electrospinning and heat-treatment processes.

FT-IR spectra for heat-treated pristine PVA nanofibers, phytoncide oil, and PVA nanofibers containing phytoncide oil before and after heat treatment are presented in Figure 6. The spectrum of pure phytoncide oil exhibits characteristic bands at 1740 cm^{-1} (C=O stretch for the acid group) and 1655 cm^{-1} (C=C conjugated diene), as shown in Figure 6(c), which do not exist in the pristine PVA nanofibers (Figure 6(d)). In contrast, the same characteristic bands of pure phytoncide oil were observed in the spectra of PVA nanofibers containing phytoncide oil before and after heat treatment, as shown in Figure 6(b) and (a), respectively. This further indicates that phytoncide oil was successfully incorporated into PVA nanofibers and was unaffected by the electrospinning process and the subsequent heat treatment.

The effect of heat treatment on the crystallinity of PVA was confirmed via FT-IR spectroscopy. In Figures 5(d) and
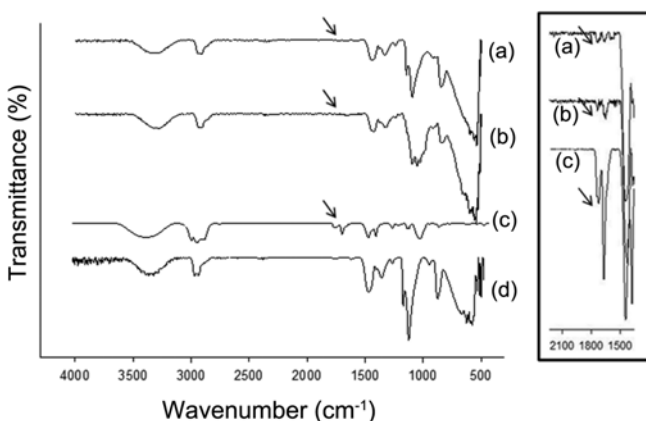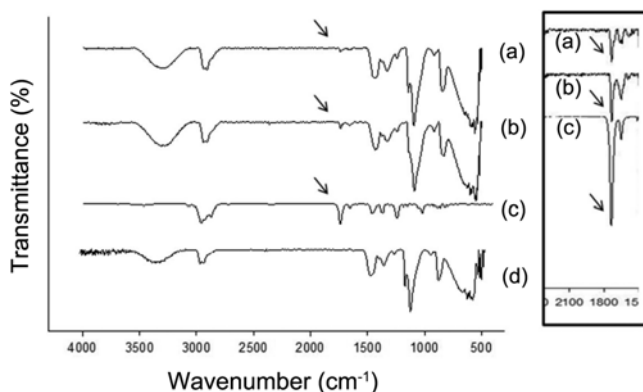
Figure 6. FT-IR spectra of (a) heat-treated electrospun phytoncide oil/PVA nanocomposite fibers, (b) untreated electrospun phytoncide oil/PVA nanocomposite fibers, and (c) pure phytoncide oil, and (d) heat-treated electrospun PVA nanofibers.
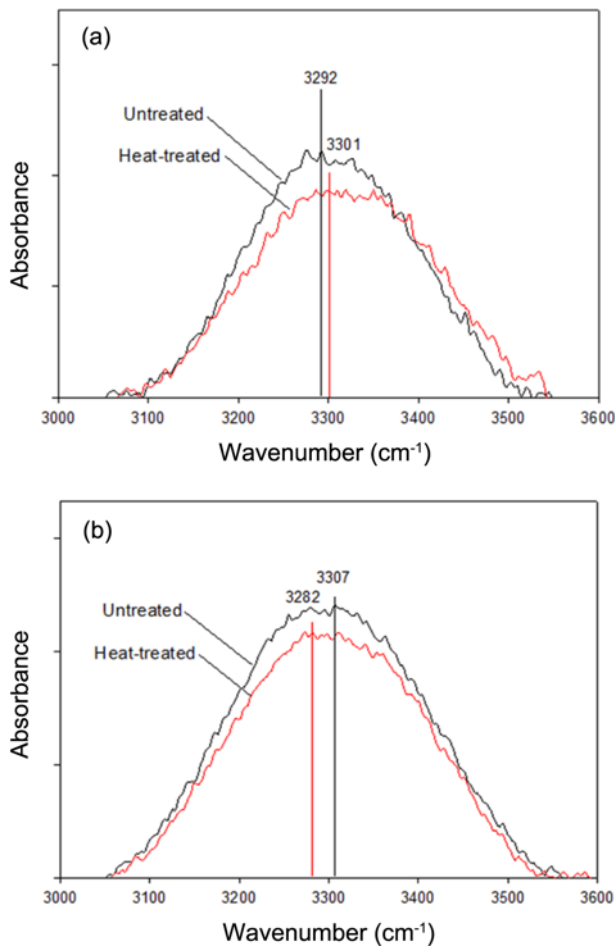
6(d), the heat-treated pristine PVA nanofibers show distinct peaks at 1143 cm^{-1}. These peaks are also present in Figures 5(a) and 6(a), *i.e.*, in the spectrum for PVA nanofibers containing essential oils after heat treatment; however, these peaks are less defined in Figures 5(b) and 6(b), *i.e.*, the spectrum for PVA nanofibers containing essential oils before heat treatment. The intensity of the peak at 1141 cm^{-1}, which is associated with the C-C stretching mode, was reported to be related to the crystallinity of PVA [35,36]. Other researchers [27,28] have also reported that the intensity of the peak at around 1140 cm^{-1} increases after heat treatment of PVA fibers owing to the higher degree of crystallinity. Based on these previous studies, the distinct peaks at 1143 cm^{-1} after heat treatment may be attributed to an increase in the crystallinity of PVA fibers.

According to Ping *et al.* [37], the absorption bands at 3100-3500 cm^{-1} are attributed to the -OH stretching vibration of the hydrogen bonds of water molecules in PVA, and the intensity of the band increases with an increase in the water content. As shown in Figure 7, in both spectra of the PVA nanofibers containing palmarosa oil and phytoncide oil, the intensity of the -OH band in the heat-treated composite fibers was slightly lower than that of their counterparts, *i.e.*, composite fibers before heat treatment, which may be attributed to the lower water content because of the higher degree of crystallinity. Our results agree well with previous studies that reported similar observations [27,38]. FT-IR results indicate that the crystallinity of PVA-based composite fibers increased after heat treatment when compared with the as-spun fibers.

Antimicrobial Efficacy of PVA Nanofibers Containing Essential Oil

Different bacteria from various sources including the environment or the surrounding skin can infect wounds. Various skin disorders, such as atopic dermatitis and acne

Figure 5. FT-IR spectra of (a) heat-treated electrospun palmarosa oil/PVA nanocomposite fibers, (b) untreated electrospun palmarosa oil/PVA nanocomposite fibers, and (c) pure palmarosa oil, and (d) heat-treated electrospun PVA nanofibers.
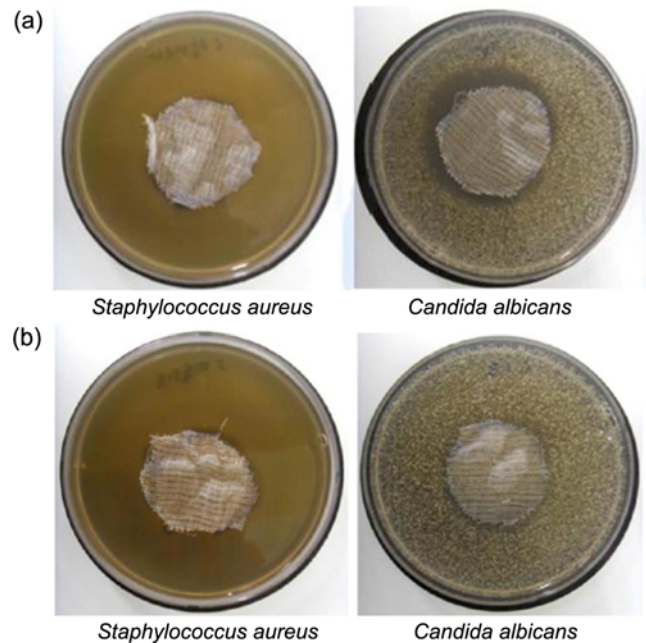
Figure 7. Changes in the FT-IR spectra of the PVA hydroxyl stretching vibration with the water content in the PVA nanofibrous membranes containing (a) palmarosa oil and (b) phytoncide oil.

Figure 8. Antimicrobial activities of electrospun PVA nanofibrous membranes containing (a) palmarosa oil and (b) phytoncide oil against *Staphylococcus aureus* and *Candida albicans*.

vulgaris, are related with secondary infection-stimulated inflammatory. Thus, prevention and/or control of infection in wounds and the surrounding areas is a desired property for wound-dressing materials. Pure PVA nanofibers showed no bacterial reduction in our previous study [9,30,39]. In this study, the antimicrobial activities of PVA nanofibers containing palmarosa oil and phytoncide oil were evaluated both qualitatively and quantitatively using two microorganisms, *Staphylococcus aureus* and *Candida albicans*, which are frequently found on human skin with dermatitis.

First, antimicrobial activities of the composite nanofibrous membranes were qualitatively evaluated according to ISO 20645:2010 (agar diffusion plate test). In this method, the level of antibacterial activity is determined by examining the extent of bacterial growth in the contact zone under the specimen and around its edges (zone of inhibition). The appearance of an inhibition zone indicates the antimicrobial activities of the specimens.

Figure 8(a) and Table 3 present the antimicrobial activities of the composite nanofibrous membranes containing palmarosa oil against *Staphylococcus aureus* and *Candida albicans*. The composite membranes containing palmarosa oil showed inhibition zones of 1.2 and 5.8 mm against *Staphylococcus aureus* and *Candida albicans*, respectively. Furthermore, there was no microbial growth underneath the specimen for both organisms, indicating strong inhibitory effects of the composite membranes against both strains.

The antimicrobial activity of the composite nanofibrous membranes containing phytoncide oil against *Staphylococcus aureus* and *Candida albicans* is presented in Figure 8(b) and Table 3. The composite membranes containing phytoncide oil exhibited an inhibition zone of approximately 1.8 mm against *Staphylococcus aureus*. No distinct zone of inhibition however was found for *Candida albicans*. Moreover, some restricted colonies were observed underneath the specimen and around its edges. These results indicate that the membranes containing phytoncide oil possessed antimicrobial effects against *Staphylococcus aureus* but not against *Candida albicans*. Thus, the qualitative assessment showed that PVA nanofibrous membranes loaded with palmarosa oil had stronger antimicrobial efficacy than PVA nanofibrous membranes loaded with phytoncide oil under the same web area density and concentration of essential oils.

Following the qualitative assessment, the antimicrobial activities of the composite membranes containing palmarosa oil and phytoncide oil were quantitatively assessed by measuring the bacterial reduction rates of the two test

Table 3. Antimicrobial activity of PVA nanofibrous membranes containing essential oils as an inhibition zone

Essential oil	Oil concentration (wt%)	Web area density (g/m^2)	Inhibition zone (mm)	
			Staphylococcus aureus	*Candida albicans*
Palmarosa oil	26	3	1.2	5.8
Phytoncide oil	26	3	1.8	0

organisms. Table 4 presents the antimicrobial activity of the composite membranes as a percentage of bacterial reduction. The membranes containing palmarosa oil at a web area density of 3 g/m^2 showed reductions of 99.9 % in both *Staphylococcus aureus* and *Candida albicans*. In contrast, the membranes containing phytoncide oil at the same web area density exhibited a reduction of 90 % in *Staphylococcus aureus* but a reduction of only 3.6 % in *Candida albicans*. The quantitative assessment confirms that the composite membranes containing palmarosa oil possessed superior inhibitory effects against both *Staphylococcus aureus* and *Candida albicans* over the membranes containing phytoncide oil. These findings also indicate that the essential oils located in the fiber core provided strong antimicrobial effects and this functionality was retained after electrospinning and heat treatment.

Evaluation of Air/Moisture Vapor Transport and Water Uptake Properties

Antimicrobial evaluations of the composite membranes containing palmarosa oil showed promising results; thus, they were selected for further evaluation of air/moisture vapor transport and water uptake properties. The air permeability, water vapor transmission rate, and water uptake of the composite nanofibrous membranes were investigated to find suitable processing conditions for creating an optimal wound-healing environment. To examine how heat treatment and web area density affect air and moisture vapor transport properties of the material, air permeability and water vapor transmission rate were assessed for PVA-based composite membranes having two levels of web area density before and after heat treatment.

Figure 9 presents the air permeability of the composite nanofibrous membranes having two levels of web area density before and after heat treatment. The air permeability of the membranes decreased as the web area density increased, and a statistical difference was observed in air permeability between the two web area densities (t-value= 4.725, p<0.05). For the same web density conditions, a slight increase was seen in the air permeability of PVA-based
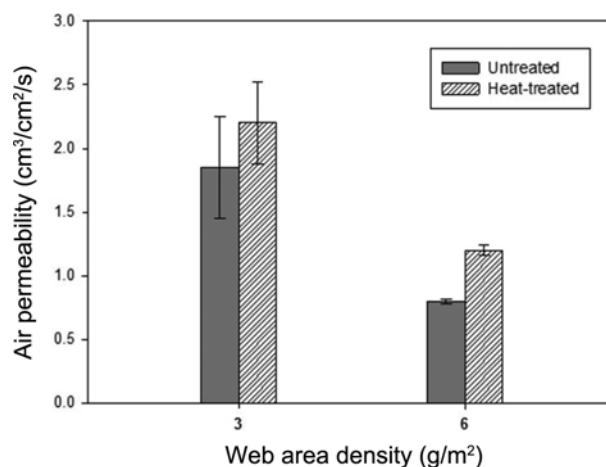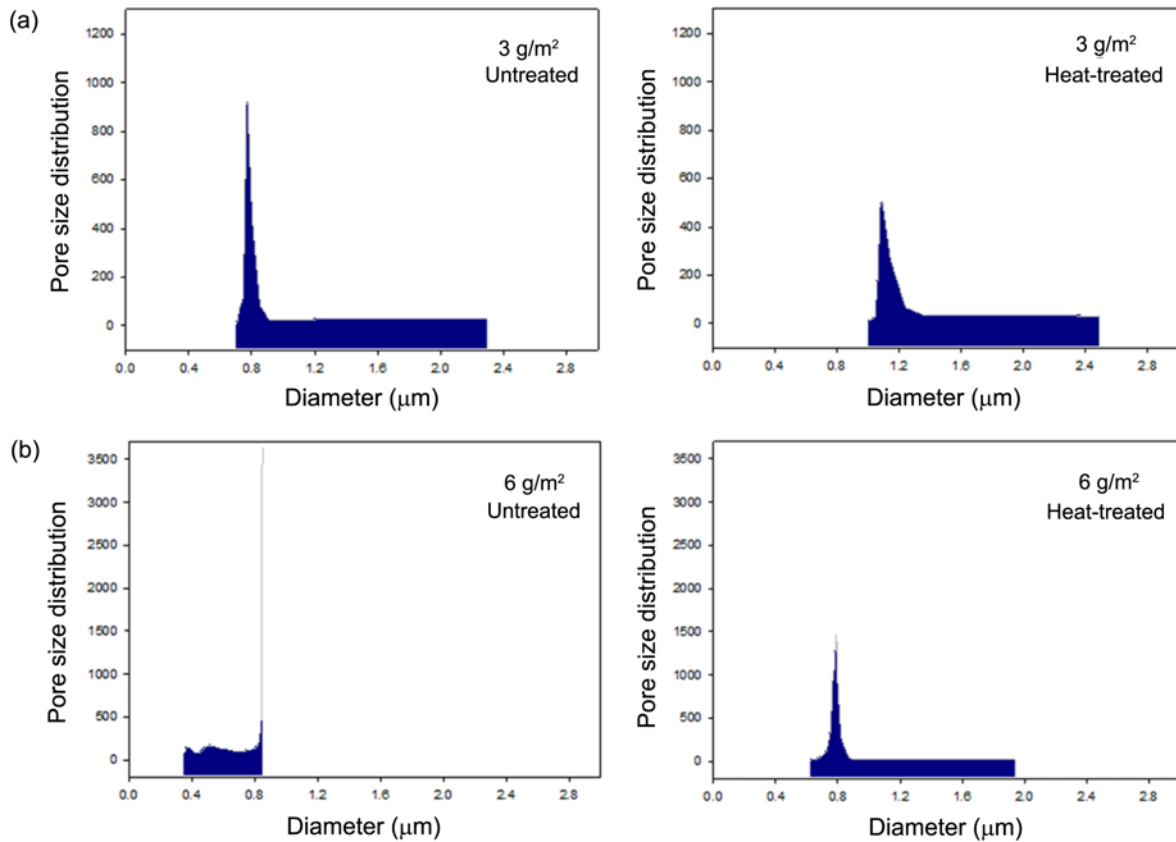
Figure 9. Air permeability of electrospun PVA nanofibrous membranes containing palmarosa oil before and after heat treatment.

composite membranes after heat treatment. A statistical difference was observed in the air permeability before and after heat treatment for the membranes having a web area density of 6 g/m^2 (t-value=3.495, p<0.05), but no significant difference was found for the membranes having a web area density of 3 g/m^2 because of heat treatment (t-value=-1.971, p>0.05), which may be related to the high variability of the specimens.

The pore size of membranes is closely associated with their air and moisture vapor permeability. Thus, pore size distribution was measured on the composite nanofibrous membranes to gain an insight on the effect of pore size on air/moisture vapor transport. Figure 10 shows the pore size distribution of the composite nanofibrous membranes having two levels of web area density before and after heat treatment. Generally, air permeability will decrease if tiny pores increase within the same area, and vice versa [40]. As shown in Figure 10, a considerable decrease in pore sizes was observed as the web area density increased. This may explain the reduction in the air permeability of membranes

Table 4. Antimicrobial activity of PVA nanofibrous membranes containing essential oils as a percentage of bacterial reduction

| Essential oil	Oil concentration (wt%)	Web area density (g/m^2)	Reduction rate of bacteria (%)	
			Staphylococcus aureus	*Candida albicans*
Palmarosa oil	26	3	99.9	99.9
Phytoncide oil	26	3	90.0	3.6

Figure 10. Pore size distribution of electrospun PVA nanofibrous membranes containing palmarosa oil before and after heat treatment; (a) 3 g/m^2 web area density and (b) 6 g/m^2 web area density.

by increasing the web area density. For the same web density conditions, there was a tendency for pore sizes to increase after heat treatment. The increase in pore sizes was more pronounced for the membranes having a web area density of 6 g/m^2. Turaga *et al.* [38] reported an increase in the pore sizes for pure PVA nanofiber webs after heat treatment, which agreed well with our findings. Since the heat-treated membranes contain a greater portion of relatively larger pores than the untreated ones, the larger pores may increase the air permeability. Thus, the increase in air permeability found in the membranes having a web area density of 6 g/m^2 may be related to the presence of larger pores.

Figure 11 presents the water vapor transmission rate of the composite nanofibrous membranes having two levels of web area density before and after heat treatment. There was a tendency for the water vapor transmission rate to decrease by increasing the web area density, which is consistent with previous research [41]. For the same web density conditions, a statistically evident increase was observed in water vapor transport for the membranes having a web area density of 6 g/m^2 after heat treatment (t-value=-16.006, $p<0.05$). There was no significant difference for the membranes having a web area density of 3 g/m^2 between the heat-treated and

untreated membranes (t-value=1.183, $p>0.05$). A comparison of pore size distribution of the as-spun and heat-treated membranes for the same web density conditions (Figure 10) shows that there was a relatively wide overlap in the pore size range between the as-spun and heat-treated membranes for the membranes having a web area density of 3 g/m^2. The as-spun membranes having a web area density of 3 g/m^2 had pore diameters ranging from 0.70 to 2.30 μm, and the pore diameters ranged from 1.01 to 2.46 μm after heat treatment. In contrast, the membranes having a web area density of 6 g/m^2 showed a substantial shift in pore size range between the as-spun and heat-treated membranes. For the as-spun membranes having a web area density of 6 g/m^2, the pore diameters ranged from 0.35 to 0.85 μm, which were between 0.63 and 1.94 μm after heat treatment. This could explain the significant increase in water vapor transport after heat treatment only for the membranes with a web area density of 6 g/m^2.

Water vapor transport is an influential factor that determines the moist environment of wounds, which is critical for the wound-healing process. The composite nanofibrous membranes with web area densities of 3 and 6 g/m^2 showed average water vapor transmission rates of 2030 and 1823 g/m^2/24 h, respectively, after heat treatment. Xu *et al.* [42] investigated
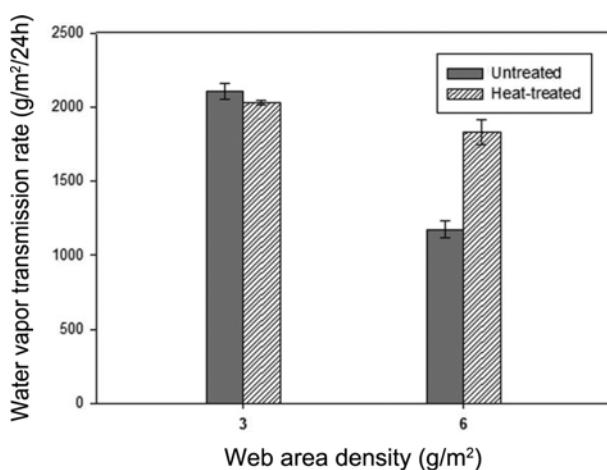
Figure 11. Water vapor transmission of electrospun PVA nanofibrous membranes containing palmarosa oil before and after heat treatment.
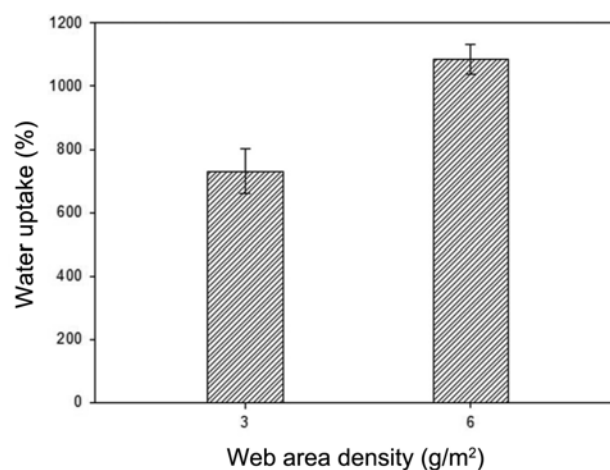
Figure 12. Water uptake of electrospun PVA nanofibrous membranes containing palmarosa oil.

the optimal water vapor transport of a dressing for wound healing using serial polyurethane membrane dressings with graded water vapor transmission rates (ranging from 50.2 to 4025.8 $g/m^2/24$ h). They found that the dressing with a water vapor transmission rate of approximately 2028.3 $g/m^2/24$ h maintained an optimal moist environment to promote wound healing. It was reported that wound dressings having water vapor transmission rates in the range of 2000-2500 $g/m^2/24$ h provided an adequate moist environment and prevented exudate accumulation [43]. Thus, the composite nanofibrous membranes with a web area density of 3 g/m^2 having an average water vapor transmission rate of 2030 $g/m^2/24$ h possessed a desirable water vapor transport property for wound-dressing applications.

An ideal wound dressing should also have the ability to absorb excessive exudates from the wound sites. Figure 12 presents the water uptake ability of the composite nanofibrous membranes having two levels of web area density. Those having web area densities of 3 and 6 g/m^2 showed average water uptake values of 731 % and 1085 %, respectively. The high water uptake ability may be related to the hydrophilic nature of PVA and the interconnected porous structure of nanofibrous membranes. The PVA-based membranes having a high web area density would have large interfiber spacing, which may hold and absorb more water than those having a low web area density. It was reported that an ideal wound dressing normally presents the water uptake in the range of 100-900 % on weight basis [44]. Thus, PVA-based composite nanofibrous membranes with a web area density of 3 g/m^2, which presented an average water uptake value of 731 %, would offer a reasonable level of water absorption and are desirable for potential wound-dressing materials.

Based on all these observations, it can be concluded that PVA nanofibrous membranes containing palmarosa oil with

a web area density of 3 g/m^2 provide suitable levels of gas and moisture vapor permeability while possessing the water uptake ability to allow exudate absorption. This indicates that nanofibrous materials that offer suitable levels of gas and moisture vapor permeability and water uptake for wound healing were obtained. Our findings also demonstrated that the air/moisture vapor transport and water uptake properties of nanofibrous membranes can be controlled by tailoring the porosity and web area density of the nanofibrous structures.

Conclusion

A new generation of wound care dressings is needed to provide a better wound-healing environment. This study aimed to develop nanofibrous membranes that satisfy essential requirements for effective wound care by integrating plant-based antimicrobials into nanofibers and optimizing the processing conditions. Essential oils as plant-derived compounds were incorporated into the core of PVA nanofibers to develop bioactive wound-dressing materials. Then, the PVA-based nanofibrous membranes were thermally treated to increase their aqueous stability. The antimicrobial efficacy, air/moisture vapor transport, and water uptake properties of the composite membranes were assessed to examine the potential for wound-dressing applications.

SEM, TEM, and CLSM analyses showed that uniform composite nanofibers in which palmarosa oil or phytoncide oil was located in the fiber core were successfully fabricated through emulsion electrospinning. Heat treatment at 170 °C for 5 min stabilized the PVA-based nanofibrous membranes against dissolution in water. FT-IR spectra indicated that the heat treatment increased the crystallinity of the fibers and suggested that the molecular structures of essential oils were maintained after electrospinning and heat treatment. Qualitative and quantitative assessments of the antimicrobial

activity of the composite membranes showed that the membranes containing palmarosa oil possessed superior antimicrobial effects against *Staphylococcus aureus* and *Candida albicans* over the membranes containing phytoncide oil. PVA nanofibrous membranes containing palmarosa oil with a web area density of 3 g/m^2 offered reasonable levels of air/moisture vapor transport for wound dressings while possessing the water uptake ability to allow exudate absorption.

Electrospun core/sheath structured nanofibrous membranes containing palmarosa oil developed in this study are permeable to water vapor and gases and exhibit strong antimicrobial effects; therefore, they have high potential in bioactive and interactive wound dressings. Our findings demonstrate that the innate structural advantages of electrospun nanofibrous membranes and antimicrobial efficacy of natural products can be combined to develop high-performance wound-dressing materials that are environment friendly and support wound healing. The release behavior of essential oils from the composite membranes and the performance of the composite membranes as bioactive wound-dressing materials *in vivo* will be further discussed in the following paper.

Acknowledgements

References

1. K. A. Rieger, N. P. Birch, and J. D. Schiffman, *J. Mater. Chem. B,* **1**, 4531 (2013).
2. S. Rajendran and S. C. Anand in "Handbook of Medical Textiles" (V. T. Bartels Ed.), pp.38-79, Woodhead Publishing Limited, Cambridge, 2011.
3. M. Abrigo, S. L. McArthur, and P. Kingshott, *Macromol. Biosci.,* **14**, 772 (2014).
4. L. Van der Schueren and K. De Clerck in "Handbook of Medical Textiles" (V. T. Bartels Ed.), pp.547-566, Woodhead Publishing Limited, Cambridge, 2011.
5. R. Sakar, A. Ghosh, A. Barui, and P. Datta, *J. Mater. Sci.: Mater. Med.*, **29**, 31 (2018).
6. K. A. Rieger and J. D. Schiffman, *Carbohyd. Polym.*, **113**, 561 (2014).
7. P. Wang and E. Mele, *Materials,* **11**, 923 (2018).
8. M. Rafiq, T. Hussain, S. Abid, A. Nazir, and R. Masood, *Mater. Res. Express,* **5**, 035007 (2018).
9. J. Jeong and S. Lee, *Text. Res. J.,* **89**, 3506 (2019).
10. H. A. Shaaban, A. H. El-Ghorab, and T. Shibamoto, *J. Essent. Oil Res.*, **24**, 203 (2012).
11. S. Khanna and J. N. Chakraborty, *Fash. Text.*, **5**, 1 (2018).
12. A. Prashar, P. Hili, R. G. Veness, and C. S. Evans, *Phytochemistry*, **63**, 569 (2003).
13. V. K. Raina, S. K. Srivastava, K. K. Aggarwal, K. V. Syamasundar, and S. P. S. Khanuja, *Flavour Fragr. J.,* **18**, 312 (2003).
14. W. Chen and A. M. Viljoen, *S. Afr. J. Bot.,* **76**, 643 (2010).
15. V. S. Dubey and R. Luthra, *Phytochemistry*, **57**, 675 (2001).
16. H. Fujimori, M. Hisama, H. Shibayama, and M. Iwaki, *J. Oleo. Sci.*, **58**, 429 (2009).
17. J. Y. Lee, S. J. Oh, M. S. Lee, J. Y. Park, J. J. Ryu, and K. H. Lee, *Fiber. Polym.*, **13**, 1209 (2012).
18. E. Ko, H. Lee, and C. Han, *J. Korean Soc. Cloth. Text.,* **43**, 288 (2019).
19. S. Raha, S. M. Kim, H. J. Lee, S. J. Lee, J. D. Heo, V. V. G. Saralamma, S. E. Ha, E. H. Kim, S. P. Mun, and G. S. Kim, *Int. J. Mol. Med.*, **43**, 393 (2019).
20. E. J. Hong, K. J. Na, I. G. Choi, K. C. Choi, and E. B. Jeung, *Biol. Pharm. Bull.*, **27**, 863 (2004).
21. J. K. Yang, M. S. Choi, W. T. Seo, D. L. Rinker, S. W. Han, and G. W. Cheong, *Fitoterapia*, **78**, 149 (2007).
22. H. J. D. Dorman and S. G. Deans, *J. Appl. Microbiol.*, **88**, 308 (2000).
23. S. Agarwal and A. Greiner, *Polym. Adv. Technol.*, **22**, 372 (2011).
24. X. Xu, X. Zhuang, X. Chen, X. Wang, L. Yang, and X. Jing, *Macromol. Rapid. Comm.*, **27**, 1637 (2006).
25. I. Sakurada, "Polyvinyl Alcohol Fibers", pp.187-209, Marcel Dekker Inc., New York, 1985.
26. M. Jannesari, J. Varshosaz, M. Morshed, and M. Zamani, *Int. J. Nanomed.*, **6**, 993 (2011).
27. M. Miraftab, A. N. Saifullah, and A. Çay, *J. Mater. Sci.*, **50**, 1943 (2015).
28. K. K. H. Wong, M. Zinke-Allmang, and W. Wan, *J. Mater. Sci.*, **45**, 2456 (2010).
29. R. C. Pasquali, M. P. Taurozzi, and C. Bregni, *Int. J. Pharm.,* **356**, 44 (2008).
30. J. Shin and S. Lee, *Fiber. Polym.*, **19**, 627 (2018).
31. S. Ramakrishna, K. Fujihara, W. E. Teo, T. C. Lim, and Z. Ma, "An Introduction of Electrospinning and Nanofibers", pp.90-102, World Scientific Publishing Co. Pte. Ltd., London, 2005.
32. I. Sriyanti, D. Edikresnha, A. Rahma, M. M. Munir, H. Rachmawati, and K. Khairurrijal, *Int. J. Nanomed.,* **13**, 4927 (2018).
33. J. Hu, M. P. Prabhakaran, X. Ding, and S. Ramakrishna, *J. Biomat. Sci.-Polym. E.*, **26**, 57 (2015).
34. J. L. Holloway, A. M. Lowman, and G. R. Palmese, *Soft Matter*, **9**, 826 (2013).
35. X. Yang, Z. Zhu, Q. Liu, and X. Chen, *J. Appl. Polym. Sci.*, **109**, 3825 (2008).
36. O. N. Tretinnikov and S. A. Zagorskaya, *J. Appl. Spectrosc.*, **79**, 521 (2012).

37. Z. H. Ping, Q. T. Nguyen, S. M. Chen, J. Q. Zhou, and Y. D. Ding, *Polymer*, **42**, 8461 (2001).
38. U. Turaga, V. Singh, R. Behrens, C. Korzeniewski, S. Jinka, E. Smith, R. J. Kendall, and S. Ramkumar, *Ind. Eng. Chem. Res.*, **53**, 6951 (2014).
39. K. Lee and S. Lee, *J. Appl. Polym. Sci.,* **124**, 4038 (2012).
40. M. E. Whelan, L. E. MacHattie, A. C. Goodings, and L. H. Turl, *Text. Res. J.*, **25**, 197 (1955).
41. S. Lee, *Fiber. Polym.*, **10**, 295 (2009).
42. R. Xu, H. Xia, W. He, Z. Li, J. Zhao, B. Liu, Y. Wang, Q. Lei, Y. Kong, Y. Bai, Z. Yao, R. Yan, H. Li, R. Zhan, S. Yang, G. Luo, and J. Wu, *Sci. Rep-UK.*, **6**, 24596 (2016).
43. Y. Chen, L. Yan, T. Yuan, Q. Zhang, and H. Fan, *J. Appl. Polym. Sci.*, **119**, 1532 (2011).
44. P. I. Morgado, A. Aguiar-Ricardo, and I. J. Correia, *J. Membrane Sci.*, **490**, 139 (2015).